Sensors and Materials, Vol. 38, No. 1 (2026) 163–172
MYU Tokyo

S & M 4292

Optimizing Responsiveness and Accuracy of Noncontact Temperature Measurement Based on Thermoreflectance

Taichi Murakami,[1] Masaki Shimofuri,[2] Toshiyuki Tsuchiya,[2] and Shugo Miyake[1*]

[1]Division of Industrial Development Engineering, Graduate School of Science and Engineering, Setsunan University, 17-8 Ikedanakamachi, Neyagawa-Shi, Osaka 572-8508, Japan
[2]Department of Micro Engineering, Graduate School of Engineering, Kyoto University, Kyoto-daigaku Katsura, Nishikyo-ku, Kyoto 615-8246, Japan

(Received November 4, 2025; accepted December 11, 2025)

Keywords: thermoreflectance, lock-in amplifier, transient temperature measurement, Ti thin-film wiring

A noncontact temperature measurement system based on thermoreflectance (TR) with a high signal-to-noise ratio (*SNR*) without temperature modulation was developed and optimized for responsiveness to achieve high-speed and accurate temperature measurement. The developed system employed a balanced photodetector and lock-in amplifier to measure minute reflectance changes in a Joule-heated Ti thin-film wiring pattern. The response characteristics of the lock-in amplifier were analyzed theoretically using a fourth-order low-pass filter model. The response time was approximately ten times the time constant (*TC*) of the filter, and *SNR* was inversely proportional to the square root of *TC*. Transient temperature measurements demonstrated that the measurement response depends strongly on *TC*, and a response time of approximately 15 ms with a temperature uncertainty of 3.3 °C was achieved by selecting the optimum *TC* value. The experimentally obtained *SNR* increased on extending *TC* to larger than the theoretical prediction, suggesting a complex noise spectrum at high frequencies.

1. Introduction

In the thermal design of electronic devices, noncontact temperature measurement with high spatial resolution is increasingly required. As device operation speeds continue to increase, for example, in power devices operating at switching frequencies in the kHz range, the assessment of temperature rise during device operation is highly important.[1–4] A change in transient temperature causes the destruction of local device parts by hot spots and a decrease in operating efficiency. Therefore, measurement techniques with higher responsiveness are needed to capture rapid temperature changes. Among various noncontact methods, the thermoreflectance (TR) technique, which utilizes the temperature dependence of optical reflectance, has the potential to achieve both high spatial resolution and responsiveness. The principle of TR temperature measurement is shown as

*Corresponding author: e-mail: shugo.miyake@edu.setsunan.ac.jp
https://doi.org/10.18494/SAM6000

ISSN 0914-4935

$$\frac{\Delta R}{R_0} = C_{TR}\Delta T \ , \tag{1}$$

where R_0 is the reflectance at the reference temperature, ΔR is the reflectance change from R_0, C_{TR} [1/°C] is the TR coefficient, and ΔT [°C] is the temperature change from the reference temperature. Because C_{TR} has a small value of the order of 10^{-3}–10^{-5} [1/°C], TR temperature measurement requires a high signal-to-noise ratio (*SNR*). However, in TR thermal imaging (TTI) using a CCD camera,[5–10] *SNR* is generally low, making it necessary to employ temperature modulation and long-time averaging (several hours), which limits the ability to perform real-time measurements. In contrast, single-point measurement using a photodiode (PD) enables measurement with a higher *SNR*, allowing shorter measurement times and real-time temperature measurement. Nevertheless, relatively slow temperature responses on the order of 1–100 s with a spatial resolution ranging from sub-μm to mm scale were measured, and the relationship between responsiveness and temperature accuracy has not been clarified in previous studies.[11–15]

In this study, we report on the evaluation of response characteristics in a TR temperature measurement system with high *SNR* that does not require temperature modulation in order to achieve high-speed and accurate temperature measurement. The developed system was used to measure transient temperature changes of Joule-heated titanium (Ti) thin-film wiring patterns in order to demonstrate the high responsiveness of temperature measurement.

2. Calculations of Responsiveness and *SNR* of TR Temperature Measurement

In the TR temperature measurement system using a photodiode, the variation in reflectance, that is, the change in the intensity of the reflected laser light, was detected using a balanced photodetector and a lock-in amplifier. The balanced detector converts the optical intensity into an electrical signal, and the lock-in amplifier measures only signals synchronized to the modulation frequency of the laser output. In this dual-phase synchronous detection, the response characteristics change because noise components and components at twice the signal frequency are removed using a low-pass filter. Equation (2) shows the step response of a fourth-order RC low-pass filter,

$$Step\ Response = 1 - \left\{ \sum_{p=1}^{4} \frac{t^{p-1}}{TC^{p-1}\left(p-1\right)!} \right\} e^{-\frac{t}{TC}} \ , \tag{2}$$

where TC denotes the time constant [s] and t represents the time [s]. Equation (3) represents the output noise [V_{rms}] of the lock-in amplifier in terms of TC,

$$Output\ noise = Input\ noise \times ENBW = Input\ noise \times \sqrt{\frac{5}{32TC}} \ , \tag{3}$$

where Input noise is the noise amplitude spectral density [V_{rms} / $\sqrt{Hz}$], including various types such as the dark current noise, the Johnson noise of the photodetector, and the laser output noise. *ENBW* [$\sqrt{Hz}$] is the equivalent noise bandwidth of the lock-in amplifier using the fourth-order low-pass filter. A smaller *TC* increases *ENBW*, allowing more noise to pass through the filter, thereby increasing the output noise. Figure 1 shows the response curves calculated from Eq. (1), where the vertical axis represents the normalized response and the horizontal axis represents time. *TC* was varied from 10 μs to 1 s. As shown, the response approaches unity after ten times the *TC* values. The time required to achieve 100% response increases proportionally with *TC*, and a higher responsiveness is achieved when *TC* is smaller. Figure 2 shows *SNR* for a given signal strength obtained from the noise variation due to *TC* in Eq. (2). The vertical axis represents *SNR* and the horizontal axis represents *TC*. *SNR* was normalized with respect to the case of *TC* = 10 μs. As *TC* increases, the output noise decreases, leading to an increase in *SNR*. These results indicate a clear trade-off between responsiveness and temperature accuracy in TR temperature

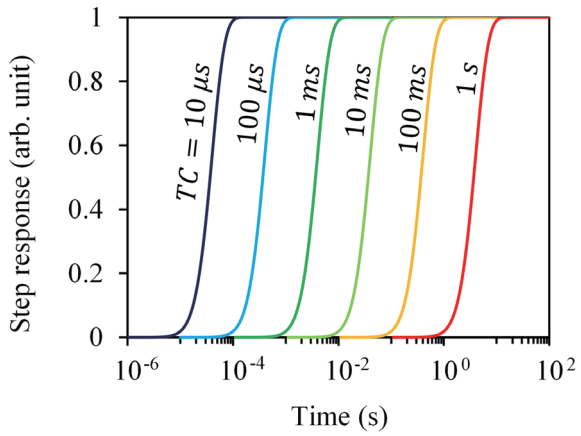

Fig. 1. (Color online) Calculation results of step response with various *TC* values of lock-in amplifier.

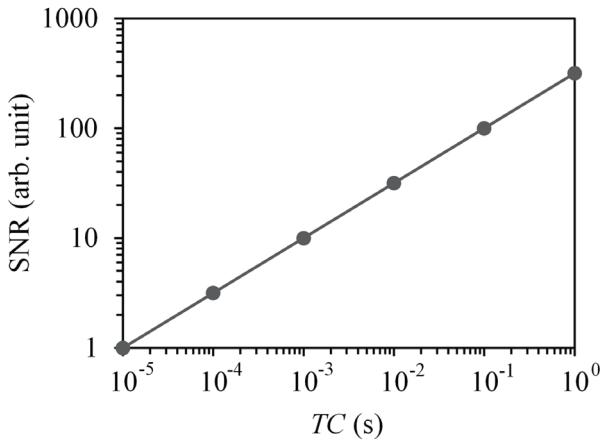

Fig. 2. Calculation results of *SNR* vs *TC* of lock-in amplifier.

measurement. Therefore, it is necessary to adjust the responsiveness determined by *TC* to a level equivalent to the temperature response time of the measurement target. The term 'optimizing responsiveness' in this study refers to this concept.

3. Experiments

3.1 Reflectance change measurement

Figure 3 shows the optical and electrical setup of the reflectance change measurement for this study. The entire setup, including the optical components, was placed on an optical surface plate and enclosed in an insulated box, maintaining room temperature. The light source was a single-mode, fiber-coupled semiconductor laser (λ = 642 nm). The beam emerging from the fiber end was collimated by a collimator and then propagated in free space. The laser beam was focused onto the sample surface mounted on the stage using a 20× objective lens with a working distance of 20 mm and a numerical aperture (NA) of 0.42. The resulting spot diameter, corresponding to the spatial resolution, was approximately 2.8 μm as determined by the image processing of the spot profile on the sample surface. The illumination laser power on the sample surface was 0.5 mW. The incident and reflected beams were separated using a nonpolarizing beam splitter and directed into a balanced photodetector (Newport Model 2307). The balanced PD comprises two photodiodes and a differential amplifier circuit, which effectively cancels out common-mode laser intensity noise—typically several times greater than the TR signal. The voltage balance between the two PD channels was fine-tuned using a neutral density (ND) filter placed in front of the PD. The laser intensity was sinusoidally modulated at 102 kHz using a function generator. Minute reflectance changes were detected through lock-in detection at the modulation frequency

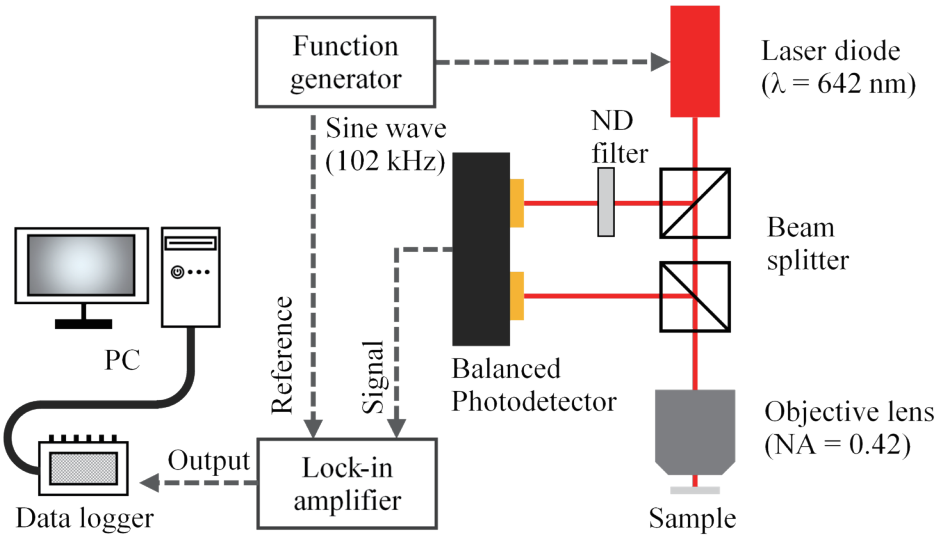

Fig. 3. (Color online) Optical and electrical setup of reflectance change measurement.

using a lock-in amplifier (SR830, Stanford Research Systems). The combination of a balanced photodetector and a lock-in amplifier enabled high-sensitivity reflectance change measurements with an improved *SNR*. The amplitude output of the lock-in amplifier is sampled at 0.1 ms intervals by the data logger, and the data is transferred to the PC.

3.2 Joule heating of Ti thin-film wiring

Figure 4 shows the Ti thin-film wiring fabricated in this study. The structure consists of two electrode pads (1000 μm square) connected by a narrow Ti line with a width of 30 μm and a length of 100 μm. A 1-mm-thick soda-lime glass substrate was ultrasonically cleaned in acetone and then spin-coated with a negative photoresist (ZPN1150 90Cp) at 3000 rpm for 30 s. The spin-coated substrate was baked at 90 °C for 2 min, followed by UV exposure in a wiring-pattern geometry (negative pattern) using a maskless lithography system (NEOARK PALET). Afterward, post-exposure bake was performed at 110 °C for 1 min. The substrate was then immersed in a developer solution (NMD-3) for 90 s to remove the unexposed resist and rinsed with pure water. Subsequently, a Ti thin film was deposited onto the patterned resist and the substrate by DC magnetron sputtering. The deposition was carried out for 60 min under the following conditions: an argon gas pressure of 0.2 Pa, a cathode power of 100 W, substrate rotation at 15 rpm at room temperature, and a deposition rate of 5 nm/min, resulting in a film thickness of 300 nm. After the deposition, the sample was immersed in acetone for 10 min to lift off the resist pattern together with the Ti layer deposited on it, yielding a wiring-patterned Ti thin film. The Ti thin film was formed on a glass substrate polished to a roughness on the order of 1 nm. Because the sputtered Ti layer has an amorphous structure, its surface is extremely

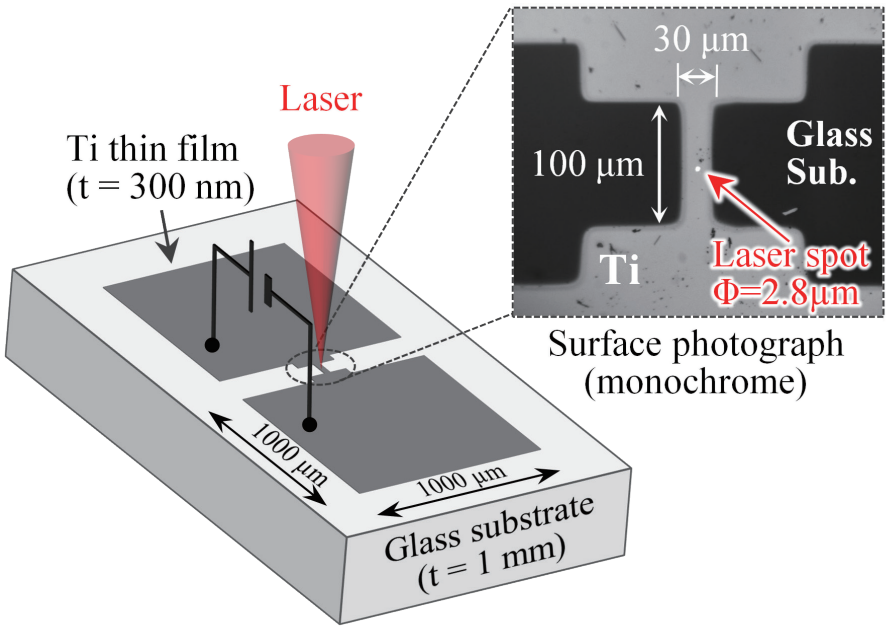

Fig. 4. (Color online) Sample overview of Ti thin-film wiring.

smooth, and therefore, the effect of scattering during laser irradiation can be neglected. Ti was selected as the material because, among the pure metals commonly used in TR measurements, it exhibits a relatively low thermal conductivity and a small volumetric heat capacity, which enable a rapid increase in temperature during Joule heating. During measurement, a voltage was applied across the two electrode pads, and the temperature increase in the narrow Ti line was monitored at the center of the line using the focused laser spot of the TR temperature measurement system. Since the laser spot diameter is approximately one-tenth the line width, the temperature distribution within the laser irradiation area was assumed to be uniform. By using a long-wavelength laser with the relatively high C_{TR} of Ti, measurement sensitivity is maximized. Figure 5 shows the step response of the voltage applied to the Ti thin-film wiring. The vertical axis represents applied voltage, and the horizontal axis represents measurement time [ms]. The voltage applied by the DC power supply (keysight E36311A) shows a delay of approximately 15 ms before reaching an output of 100% . The power supply is equipped with an output filter that suppresses ripple and noise, and the increase time of the output voltage depends on this filtering circuitry.

4. Results and Discussion

Figure 6(a) shows the measured reflectance change as a function of Joule heating power. The vertical axis represents the reflectance change $\Delta R/R_0$ [10^{-3}] and the horizontal axis represents the heating power [mW]. The measurement was performed with TC = 100 μs. For each heating power, the average $\Delta R/R_0$ during the 1 s constant heating period is plotted. The standard deviation of $\Delta R/R_0$ was 1.8×10^{-4}. $\Delta R/R_0$ decreased linearly with increasing heating power, and the residual standard deviation of the linear fit (dashed line) was 7.8×10^{-5}. Figure 6(b) shows the temperature change ΔT converted from the $\Delta R/R_0$ data using the literature value of C_{TR}. The vertical axis represents the temperature change ΔT (°C) and the horizontal axis represents the heating power (mW). The applied C_{TR} value was -5.76×10^{-5} (1/°C).[16] The temperature increased linearly with the heating power, and the maximum temperature increase of the Ti thin film line reached +131.9 °C at 28.8 mW. The temperature uncertainty for each data point was

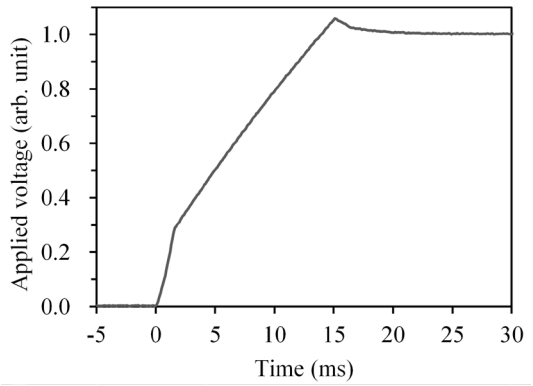

Fig. 5. Step response of voltage applied to Ti thin-film wiring.

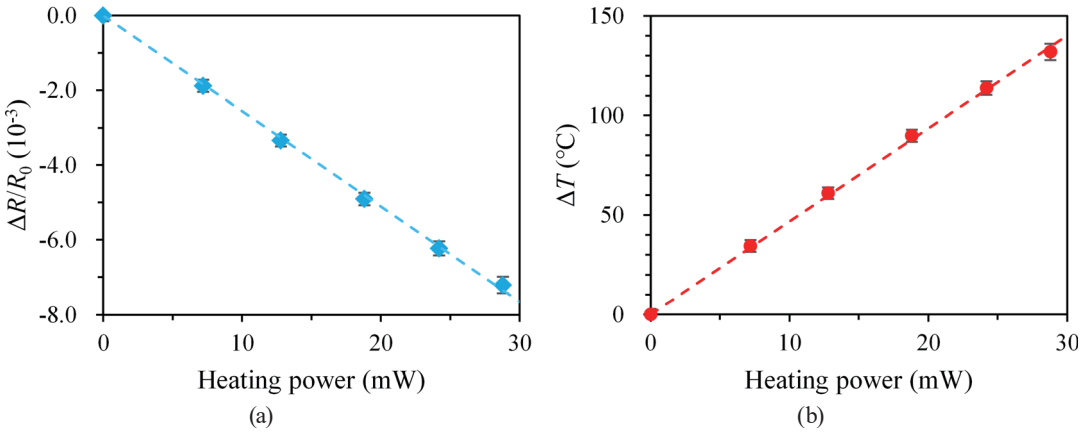

Fig. 6. (Color online) (a) Reflectance change with constant heating power. (b) Temperature change with constant heating power.

estimated to be 3.3 °C, and the residual standard deviation of the fitted line (dashed line) was 1.43 °C. These results indicate that the temperature dependence of the reflectance of the Ti thin-film wiring exhibits high linearity in reflectance change from room temperature to approximately 200 °C. This is consistent with previously reported results for pure metals.[17,18]

Figure 7 shows the measurement results of reflectance change with transient temperature at a heating power of 7.2 mW. The left vertical axis represents the reflectance change $\Delta R/R_0$ (10^{-3}), the right vertical axis represents the applied voltage (V), and the horizontal axis represents the measurement time (ms). The measurement time was defined such that 0 ms corresponds to the start of heating. The reflectance change measured at constant room temperature before heating is plotted at negative time values, whereas the data acquired after heating begins are shown at positive time values. The plotted $\Delta R/R_0$ corresponds to the measurements obtained at various *TC* values of 10 μs to 100 ms. The increase in the measured $\Delta R/R_0$ became slower with increasing *TC*. For *TC* values of (d) 10 and (e) 100 ms, $\Delta R/R_0$ had not yet reached a steady state even at 30 ms. In contrast, for *TC* values of 10 and 100 μs, although the $\Delta R/R_0$ data exhibited larger fluctuations, they appeared to reach steady-state values within 15 ms. However, the response at *TC* = 1 ms showed a slight delay of 10 ms. These behaviors are consistent with the relationship between *TC* and output responsiveness described in Sect. 2, where the output requires approximately ten times the *TC* to reach 100%. Therefore, when *TC* = 1 ms, the expected response time of 10 ms is comparable to the voltage increase time of 15 ms, resulting in a notable delay in the measured $\Delta R/R_0$ compared with the faster *TC* settings of 10 and 100 μs. No significant difference in $\Delta R/R_0$ was observed when the applied voltage increase was approximately 1.4 ms. $\Delta R/R_0$ measured at *TC* = 10 μs indicates that the response to the voltage increase remained almost unchanged compared with when *TC* = 100 μs. Therefore, the transient temperature of the Ti thin film increases at a rate nearly identical to the rate of increase in applied voltage, and the TR temperature measurement system developed in this study was confirmed to have a response time of up to 15 ms with a time resolution of 0.1 ms.

Figure 8 shows *SNR* and the uncertainty of $\Delta R/R_0$ at constant room temperature. The vertical axis (left) represents *SNR*, the vertical axis (right) represents the uncertainty of $\Delta R/R_0$, and the

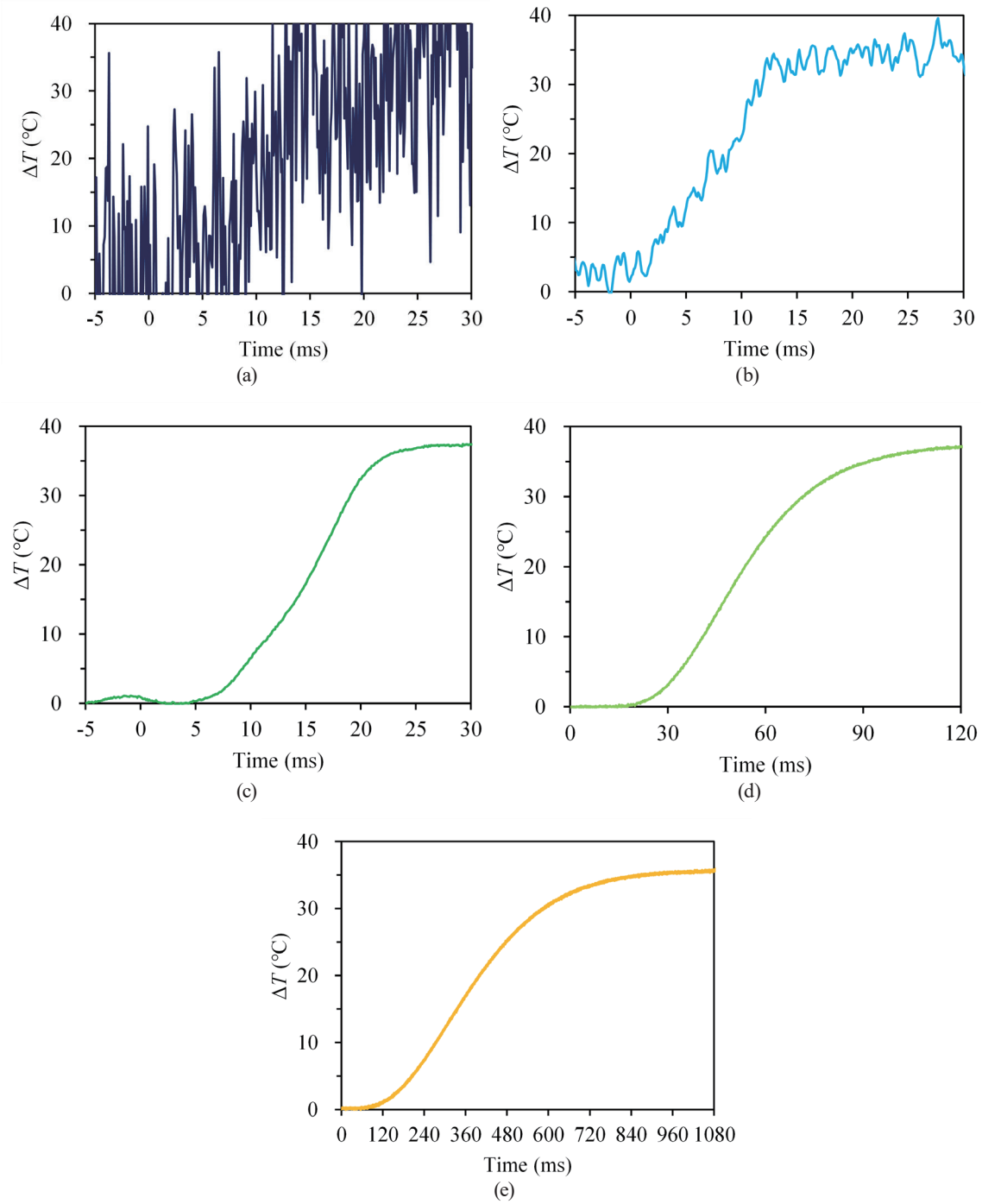

Fig. 7. (Color online) Reflectance change with transient temperature at heating power of 7.2 mW and (a) *TC* = 10 µs, (b) *TC* = 100 µs, (c) *TC* = 1 ms, (d) *TC* = 10 ms, and (e) *TC* = 100 ms.

horizontal axis represents *TC*. *SNR* is normalized by the obtained value at *TC* = 10 µs. The standard deviation of $\Delta R/R_0$ measured over a 10 s period at constant room temperature is employed at each *TC*. *SNR* increased with *TC*. However, the increase in *SNR* associated with the increase in *TC* was generally larger than the calculated results described in Sect. 2. In particular,

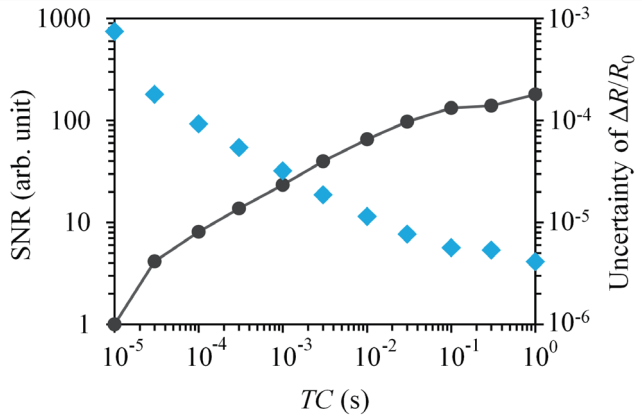

Fig. 8. (Color online) *SNR* of measurement results and uncertainty of $\Delta R/R_0$ at room temperature.

a pronounced drop was observed at $TC \leqq 30$ μs. This tendency suggests that the noise originating from the laser output, photodetector, and lock-in amplifier is more widely distributed in the high-frequency region. In other words, the noise spectrum does not simply follow a √Hz dependence but likely exhibits a more complex frequency distribution. Furthermore, the relatively small slope of the *SNR* increase at $TC \geqq 100$ ms can be attributed to the low uncertainty resulting from the sufficiently high sampling rate and short measurement time relative to the output low-frequency noise. The uncertainty of $\Delta R/R_0$ increases as *TC* decreases with improving responsiveness. This result aligns with the calculations and trends in Sect. 2. and is likely due to the increased output noise of the lock-in amplifier. Since the C_{TR} of most pure metals is on the order of 10^{-4}–10^{-5} (1/°C), achieving a temperature accuracy of 1 °C requires a *TC* of at least 100 μs.

5. Conclusions

In this study, a noncontact TR temperature measurement system in which the reflected laser beam is detected by a photodiode with high *SNR* was developed, and the relationship between responsiveness and temperature accuracy was evaluated. Theoretical calculations based on a fourth-order low-pass filter model clarified that the output response of the lock-in amplifier requires ten times the *TC* to reach 100%, and that *SNR* decreases in proportion to the square root of *TC*. Using the developed system, temperature measurements of a Joule-heated Ti thin-film wiring surface were performed. The reflectance and temperature changes showed linear relationships with heating power. Transient temperature measurements demonstrated that the step response becomes slower as *TC* increases, and a response time of approximately 15 ms was achieved at $TC = 10$ and 100 μs. The experimentally observed *SNR* increase with increasing *TC* was larger than the theoretical prediction, suggesting that the noise components of the laser, photodetector, and lock-in amplifier are distributed nonuniformly in the high-frequency region. These findings quantitatively clarify the trade-off between responsiveness and temperature accuracy in TR temperature measurement and provide practical guidelines for optimizing measurement conditions for fast transient thermal phenomena in micro- and nanoscale devices.

To achieve both high responsiveness and temperature accuracy, improving measurement sensitivity will be highly effective. Recently, methods based on optical interference[19,20] and the wavelength dependence of C_{TR}[21,22] have been reported to achieve high sensitivity (~10^{-3} order). Using these methods, real-time temperature measurement combining sub-millisecond response time with a temperature uncertainty below 1 °C is expected.

Acknowledgments

Part of this research was supported by a JST Grant-in-Aid for Scientific Research (Project No. 24H00284). The authors would like to express their sincere gratitude to Associate Professor Mitsuhiro Horade of Setsunan University for his valuable assistance in the fabrication of the wiring patterns.

References

1 Y. Song, P. A. Schirmer, P. Schreivogel, K. Zhang, H. Wang, and F. Blaabjerg: IEEE Trans. Power Electron. **40** (2025) 7251. https://doi.org/10.1109/TPEL.2025.3530148
2 L. Dupont, Y. Avenas, and P. O. Jeannin: IEEE Trans. Ind. Appl. **49** (2013) 1599. https://doi.org/10.1109/APEC.2012.6165817
3 G. Pavlidis, D. Kendig, L. Yates, and S. Graham: Proc. ITherm. (2018) 208. https://doi.org/10.1109/ITHERM.2018.8419649
4 S. Martin-Horcajo, J. W. Pomeroy, B. Lambert, H. Jung, H. Blanck, and M. Kuball: IEEE Electron Device Letters, **37** (2019) 1197. https://doi.org/10.1109/LED.2016.2595400.
5 M. G. Burzo, P. L. Komarov, and P. E. Raad: IEEE Trans. Compon. Packaging. Manuf. Technol. **28** (2005) 637. https://doi.org/10.1109/TCAPT.2005.859738
6 B. Vermeersch, J. Bahk, J. Chirstofferson, and A. Shakouri: J. Appl. Phys **113** (2013) 1. https://doi.org/10.1063/1.4794166
7 P. M. Mayer, D. Lüerßen, R. J. Ram, and J. A. Hudgings: J. Opt. Soc. Am. A **24** (2007) 1156. https://doi.org/10.1364/JOSAA.24.001156
8 T. Zhu, D. H. Olson, P. E. Hopkins, and M. Zebarjadi: Rev. Sci. Instrum. **91** (2020) https://doi.org/10.1063/5.0024476
9 D. U. Kim, C. B. Jeong, J. D. Kim, K. Lee, H. Hur, K. Nam, G. H. Kim, and K. S. Chang: Sensors **17** (2017) 2774. https://doi.org/10.3390/s17122774
10 R. Mckenna, D. Mickus, S. Naimi, C. Murphy, M. Mcdermott, S. Corbett, D. Mccloskey, and J. F. Donegan: OSA Continuum **4** (2021) 1271. https://doi.org/10.1364/OSAC.422429
11 T. Murakami, M. Shimofuri, T. Tsuchiya, and S. Miyake: Sens. Mater. **36** (2024) 3445. https://doi.org/10.18494/SAM5165
12 A. El Helou, P. E. Raad, and P. Komarov: Proc. SEMI-THERM (2018) 161. https://doi.org/10.1109/SEMI-THERM.2018.8357368
13 Y. Shimizu, J. Ishii, and T. Baba: Jpn. J. Appl. Phys. **46** (2007) 3117. https://doi.org/10.1143/JJAP.46.3117
14 Y. Liu, A. Mandelis, M. Choy, C. Wang, and L. Segal: Rev. Sci. Instrum. **76** (2005) 084902. https://doi.org/10.1063/1.2001673
15 S. Dilhaire, S. Grauby, and W. Claeys: Appl. Phys. Lett. **84** (2004) 822. https://doi.org/101063/1.1645326
16 P. E. Raad, P. L. Komarov, and M. G. Burzo: Electronics Cooling **14** (2008) 28.
17 T. Favaloro, J.-H. Bahk, and A. Shakouri: Rev. Sci. Instrum. **86** (2015) 024903. https://doi.org/10.1063/1.4907354
18 B. Meng, Y. Ma, X. Wang, and C. Yuan: J. Appl. Phys. **134** (2023). https://doi.org/10.1063/5.0164110
19 C. Shi, X. Wang, Q. Zheng, J. Maroske, and D. Thompson: Opt. Express **32** (2024) 1003. https://doi.org/10.1364/OE.511938
20 M. S. Tekmedash and A. Reihani: Sens. Actuators, A **379** (2024) 115949. https://doi.org/10.1016/j.sna.2024.115949
21 T. Murakami, M. Shimofuri, T. Tsuchiya, and S. Miyake: J. JSEM. **25** (2025) 29 (in Japanese). https://doi.org/10.11395/jjsem.25.29
22 H. Zhang, S. Wen, and A. Bhaskar: Appl. Phys. Lett. **114** (2019) 151902. https://doi.org/10.1063/1.5087011